Contents lists available at ScienceDirect

Journal of the Mechanical Behavior of Biomedical Materials

Material and mechanical behavior of bracket fungi context as a mechanically versatile structural layer

Ihsan.S. Elnunu [a], Jessica.N. Redmond [a], Bryn.T.M. Dentinger [b], Steven.E. Naleway [a],[*]

[a] Department of Mechanical Engineering, University of Utah, Salt Lake City, UT, USA
[b] Natural History Museum of Utah and School of Biological Sciences, University of Utah, Salt Lake City, UT, USA

ARTICLE INFO

ABSTRACT

Bracket fungi sporocarps present promising environmentally friendly alternatives to harmful and wasteful structural applications with their high strength-to-weight ratio mechanical properties. Kingdom *Fungi* is estimated to have over three million species, yet only 4% of the species have been described by mycologists, and their mechanical behavior has been under-explored. This work aims to characterize the material behavior and mechanical properties of bracket fungi as a whole through micro-mechanical tensile testing combined with microstructural imaging and analysis of two representative species. The context layer from three distinctive fresh bracket sporocarps is used in this study. At the microstructure level, the bracket fungi have a preferred alignment in the hyphal network, which correlates to the radial direction. The bracket fungi exhibit an anisotropic mechanical behavior with higher ultimate tensile strength and elastic modulus in the radial direction, while the strain to failure is higher in the transverse direction. However, the bracket fungi exhibit an isotropic energy absorption, or toughness, behavior, with no statistically significant difference between the radial and transverse directions. The characterization of anisotropic mechanical properties and isotropic energy absorption will inspire the exploration of bracket fungi as a viable alternative to applications in various industries, such as aerospace and agriculture.

1. Introduction

According to one estimate, Kingdom *Fungi* has between 2.2 and 3.8 million species, but mycologists have only described around 150,000 species (Hawksworth and Lücking, 2017). Mycologists from different geographical regions are still discovering and studying more species to add to the ever-growing field of mycology and mycology-focused engineering (Hawksworth and Lücking, 2017; Lücking et al., 2021). Fungi have been an integral part of the human diet and disease treatment for centuries (Valverde et al., 2015). Beyond their common uses, the resilient fungi adapt to geographically different regions, climates, and different food sources using robust structures (Sterflinger et al., 2012; Naranjo-Ortiz and Gabaldón, 2019). Due to the robustness of their structures, researchers have specifically evaluated and studied mycelium-based composites and the fungal sporocarps' mechanical behavior in the past few years (Porter and Naleway, 2022; Müller et al., 2021; Pylkkänen et al., 2023; Klemm et al., 2024). Due to their significant mechanical properties, fungi have been a trending topic as an environmentally friendly alternative to environmentally harmful and wasteful applications in aerospace, clothing, agriculture, and structural materials (Ghazvinian and Gürsoy, 2022; Meyer et al., 2020; Amobonye et al., 2023; Ongpeng et al., 2020). While fungi cover a range of fungus types, filamentous fungi are of particular interest because of their macrostructural mechanical properties (Porter and Naleway, 2022; El-Enshasy, 2007; Wösten, 2019; Bueno and Silva, 2014; Porter et al., 2023; Ogawa et al., 2012).

Filamentous fungi comprise hyphae as their basic cellular unit with chitinous cell walls (Islam et al., 2017; Zabel and Morrell, 2020). Filamentous fungi reproductive sporocarps range about two orders of magnitude in strength, from soft-textured and low-strength sporocarps similar to a dish sponge to hard-textured and high-strength sporocarps similar to hardwood (Porter and Naleway, 2022; Müller et al., 2021; Klemm et al., 2024; McGarry and Burton, 1994). Many high-strength sporocarps are found in various genera in the order Polyporales and are commonly known as "polypores" (Richter et al., 2015). Polypores are unique because they have many densely arranged tubes with fertile inner surfaces that form and release spores (Miettinen et al., 2012; Vlasenko, 2013; Kauserud et al., 2008). Polypores with large, stalkless,

---

and woody sporocarps are also known as bracket fungi (Yoshimoto, 1970; Bishop, 2020). These bracket fungi grow on fallen and standing woody tree trunks and have a strong mechanical attachment to the tree, which requires tools such as a hammer and chisel or significant human force to remove them (Müller et al., 2021; Vlasenko, 2013; Cristini et al., 2023). The physical strength of the woody bracket sporocarp is attributed to its cellular structure (Pylkkänen et al., 2023).

Bracket fungi sporocarps are lightweight with a hard bracket or shelf-like shape and woody texture (Müller et al., 2021; Bishop, 2020; Zjawiony, 2004). Looking at the cross-section, bracket fungi sporocarps have three distinct layers: 1) crust, 2) context, and 3) tubes, as seen in Fig. 1. The crust is a thin, rigid layer presumably protecting the sporocarp (Klemm et al., 2024; ud-Din and Mukhtar, 2019; Petersen, 1987). The context layer is a fleshy tissue sandwiched and enclosed between the crust and tube layers (Porter et al., 2023). The context layer's thickness varies depending on the species, but it is usually the thickest layer containing the structure's bulk to support the sporocarp's structure (Müller et al., 2021; Porter et al., 2023; Hattori et al., 2014). Although the context is dense, formed from hyphae, and comprises most of the sporocarp tissue, it keeps the sporocarp lightweight (Müller et al., 2021; Porter et al., 2023; Schmidt et al., 2023; Elsacker et al., 2019). In many species, such as those of the genus *Ganoderma*, the size of the sporocarp is directly related to the thickness of the context (Luangharn et al., 2020; Glen et al., 2009; Wang et al., 2012a; Xing et al., 2018; Ryvarden, 2000). The tube layer is the bottom layer of the sporocarp, which is the part facing towards the ground (Müller et al., 2021; Klemm et al., 2024; Porter et al., 2023). The parallelly arranged tubes are normal to the context to allow the spores to drop out of the pores by gravity (Money and Fischer, 2009). Considering the different roles of each layer, understanding the mechanical behavior of the context layer, which comprises most of the sporocarp tissue, is vital to explaining the mechanical properties of bracket structure.

Experimental mechanics research on fungal sporocarps is still preliminary. While the structural and mechanical properties of fungal sporocarps vary for different species, the current research findings are species-specific (Porter and Naleway, 2022; Müller et al., 2021; Pylkkänen et al., 2023; Klemm et al., 2024). To fully understand the mechanical and microstructural behavior of bracket sporocarps, researching multiple species is paramount to capture natural variation and identify common themes. Therefore, mechanically testing and comparing the context layer of multiple species due to its abundance, support role, woody texture, and dense hyphae network in the sporocarp can allow a better understanding of all mechanical behavior and microstructure and better highlight the significant structural elements that provide these properties in bracket sporocarps.

In this paper, we studied three bracket fungi sporocarps from two distinct species of bracket fungi to describe the general material and mechanical behavior of bracket sporocarps via micro-mechanical testing coupled with microstructural imaging and analysis. The mechanical and material characterization of bracket context allows for a comprehensive understanding of the bracket's structural and physical properties. The characterization may lead to exploring a sustainable, green material alternative in various fields and inspire more bioinspired designs.

2. Materials and methods

2.1. Sample collection and DNA extraction and barcoding

Three bracket fungi sporocarps were foraged from the Wasatch Mountain Range in northern Utah, United States, growing on fallen dead trees. The bracket fungi were kept fresh and hydrated from the day they were obtained to testing in a controlled and refrigerated environment, with no longer than 14 days before testing.

DNA was extracted from the context layer using a lysis buffer and incubation process to confirm the identity of the fungus, and then universal DNA barcode sequences from the nuclear ribosomal internal transcribed spacers (ITS) were generated. The ITS was amplified using the Agaricomycetes-specific PCR primers, ITS-8F (5′-AGTCGTAA-CAAGGTTTCCGTAGGTG-3′) and ITS-6R (5′-TTCCCGCTTCACTCGCAGT-3′) (Dentinger et al., 2010). The DNA was cleaned using a combination of exonuclease I and shrimp alkaline phosphatase, then Sanger sequencing was performed at the DNA sequencing core at the University of Utah (Bradshaw et al., 2022). Voucher specimens are deposited in the fungal collection of the Garrett Herbarium, University of Utah (UT).
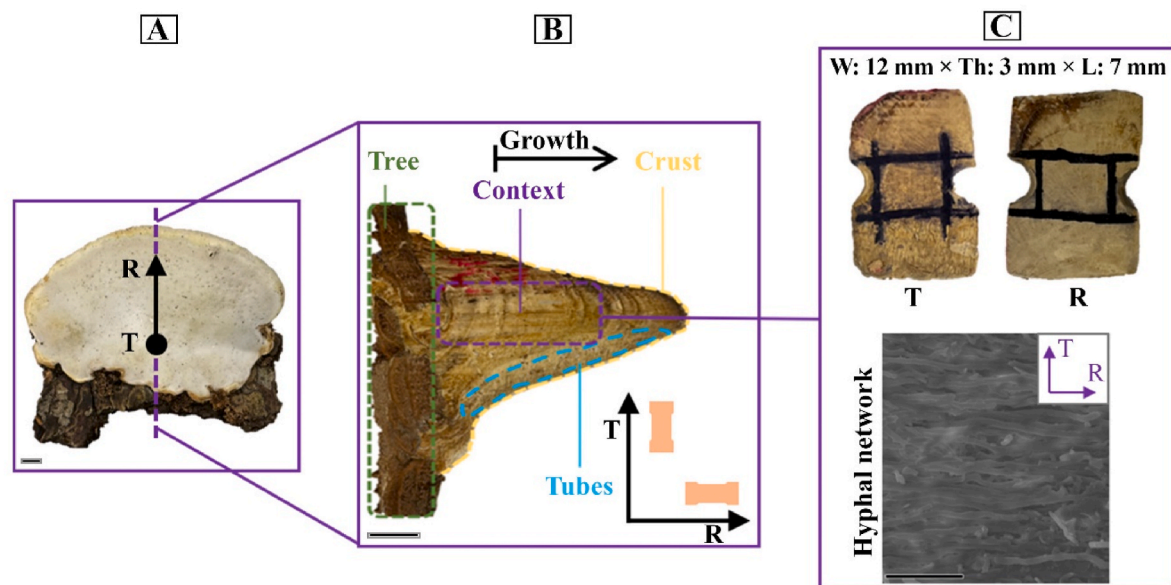
Fig. 1. Schematic showing the different layers in bracket fungi, hierarchical structure, tensile test samples, and coordinate system used to define directionality for mechanical tests and microstructure analysis. **(A–B)** The radial (R) direction is associated with the bracket fungi's growth direction, while the transverse (T) direction is perpendicular to the growth direction. **(B)** The cross-section of bracket fungi shows three layers: crust, context, and pores. **(C)** The tensile test samples for the R and T directions and the hyphal network at the microstructure show the hyphae aligned in the radial direction. Scale bars in **(A)** and **(B)** = 1 cm, while the scale bar in **(C)** = 50 μm.

Each of the three bracket fungi was also processed into smaller sections depending on the growth direction, radial (along the growth direction), and transverse (against the growth direction) while maintaining the integrity of the context layer for the following material and mechanical testing techniques. The preparation process involved isolating the context layer and avoiding weak interfaces.

2.2. Chemical characterization

Fourier-transform infrared spectroscopy (FTIR) was used to compare the chemical compositions of the three bracket sporocarps. A Thermo Scientific Nicolet iS50 FTIR Spectrometer with OMNIC software (Thermo Fisher Scientific, Waltham, MA, USA) was used for the chemical composition comparison. One FTIR sample per sporocarp was used to collect the three spectra. A sample from each bracket fungi sporocarp was placed onto an attenuated total reflection window and securely compressed into place by a diamond tip to collect the spectra data. The experiment was set up to collect 32 scans with a data spacing of 0.482 cm^{-1}. The spectra wavenumbers range for the collected samples was 800–3600 cm^{-1}, and the absorbance range was 0.028–0.23.

2.3. Uniaxial micro-mechanical testing

Uniaxial tensile tests were performed on the fresh and hydrated sporocarp context layer to assess their mechanical properties in a mode similar to pull-off predation (Zhao et al., 2022). A Psylotech MicroTest System (Psylotech Incorporated, Evanston, IL, USA) equipped with a 434 N load cell was used to conduct the uniaxial tensile tests until fracture. All tested context samples had a span of 7 mm between the grips and were fixed into clamps with a 1.2 Nm torque to avoid slippage. All uniaxial tensile tests on the context were performed with a displacement speed of 25 μm/s. For each sporocarp, two groups were tested based on orientation from the fungus's context, radial ($n = 9$) and transverse ($n = 9$). These orientations were chosen due to the fungus's growth direction, where the radial direction is the growth direction, and the transverse direction is the perpendicular direction to the bracket fungus's growth. The stress and strains were calculated from the force-displacement data output from the tensile test. Using the stress-strain curves, the elastic modulus, E, ultimate tensile strength, σ_{uts}, strain to failure, ε_f, and toughness were calculated in MATLAB. E was calculated by finding the stress-strain slope, while σ_{uts} was calculated by finding the maximum stress before failure. The strain to failure was defined as the maximum percent strain at failure. The toughness was defined as the area under the stress-strain curve, interpreted as the energy absorbed during deformation per unit volume. A total of 54 samples were used for the uniaxial micro-mechanical tensile test and the mechanical properties calculations.

2.4. Microstructure imaging and characterization

The context layer of each sporocarp was examined by microstructural imaging before and after mechanical testing using scanning electron microscopy (SEM) (FEI Quanta 600 FEG-ESEM, Hillsboro, OR, USA) to characterize the hyphae alignment orientation, diameters, and density. For the microstructure imaging and characterization, all samples were secured on aluminum stubs via conductive PELCO isopropanol-based graphite paint and then coated with gold-palladium. SEM imaging was conducted using an accelerating voltage of 20 kV and a spot size of 5 nm. All characterization analyses were performed using ImageJ software (Schneider et al., 2012).

For pre-test characterization, three samples ($n = 3$) were prepared from each sporocarp. Images were collected from two distinct areas within each sample, resulting in a total of six images per sporocarp to ensure consistent measurements. For hyphae characterization, 20 individual hypha were measured per image for the hyphae alignment

orientation and diameter, resulting in 120 measurements. To measure the density, the threshold was adjusted to account for all the hyphae in the image. Then, the percentage of the area the hyphae cover was measured, resulting in six measurements per sporocarp.

For post-test characterization, three samples ($n = 3$) were prepared from the transversely mechanically tested samples and were imaged from the top view. Two distinct images were collected per sample in the region between the clamps and fracture point for each sample. The process used in the pre-test characterization for hyphae alignment orientation characterization was used. Similarly, a total of 120 measurements for each sporocarp were recorded for the hyphae alignment.

2.5. Statistical analysis

Statistical analyses were performed using MATLAB software. Statistical significance was determined by performing two-tailed, two-sample t-tests on the mechanical properties data from the micro-mechanical uniaxial tensile test, and the microstructure characterization data from SEM images. The significance level for all presented data was set at α = 0.05.

3. Results and discussion

3.1. DNA extraction and barcoding

DNA sequencing confirmed the bracket fungi to belong to two distinct species: 1) *Ganoderma applanatum* (Polyporales: Polyporaceae) (Fig. 2 (A)), also known as artist's conk, which is a close relative of one of the most popular species of *Ganoderma* known for medicinal use (Jo et al., 2009; Jeong et al., 2008; Luo et al., 2016; Cheng et al., 2024); 2) *Fomitopsis ochracea* (Polyporales: Fomitopsidaceae) (Fig. 2 (B and C)), a recently discovered bracket fungus found in northern North America (Ginns, 2017; Haight et al., 2016, 2019). The DNA sequencing of *Ganoderma applanatum* is 100% identical to 59 sequences in GenBank; 42 are identified as *G. applanatum*, 1 as G *adspersum*, 1 as G *lipsiense*, and 15 as unidentified. The *Fomitopsis ochracea*'s DNA sequence is most closely related to sequences of *Fomitopsis ochracea*, (see supplement). DNA sequences generated to validate species identification are submitted to GenBank (Accessions PQ700181, PQ700179, PQ700180). Garrett Herbarium UT-M accession numbers for the voucher specimens are UT-M0002380 for *Ganoderma applanatum* and UT-M0002381 and UT-M0002382 for the two *Fomitopsis ochracea*. *Ganoderma applanatum* and the two *Fomitopsis ochracea*, will be referred to as *G. applanatum*, *F. ochracea* (I), and *F. ochracea* (II), respectively, throughout the manuscript.

3.2. FTIR chemical characterization

FTIR was used to collect the spectra for the three bracket fungi sporocarps as shown in Fig. 2 (D). The figure shows consistent peaks for each of the spectra curves for *G. applanatum*, *F. ochracea* (I), and *F. ochracea* (II). The similar peaks demonstrate that the chemical composition is the same for all three tested samples. All the chemical components expected in fungi are present due to the same chemical composition of OH, NH, lipids, proteins, chitin, and polysaccharides (Naumann et al., 2015; Mohaček-Grošev et al., 2001). Of note, the chemical composition and peaks are consistent with previous reports on the same and other bracket fungi in the Agaricomycetes class (Kaya et al., 2015; Wang et al., 2012b). The FTIR spectra confirm that there were no significant chemical changes between the three tested sporocarps.

3.3. Uniaxial micro-mechanical testing

3.3.1. Ultimate strength and elastic modulus

The tensile micro-mechanical testing was done on the context layer
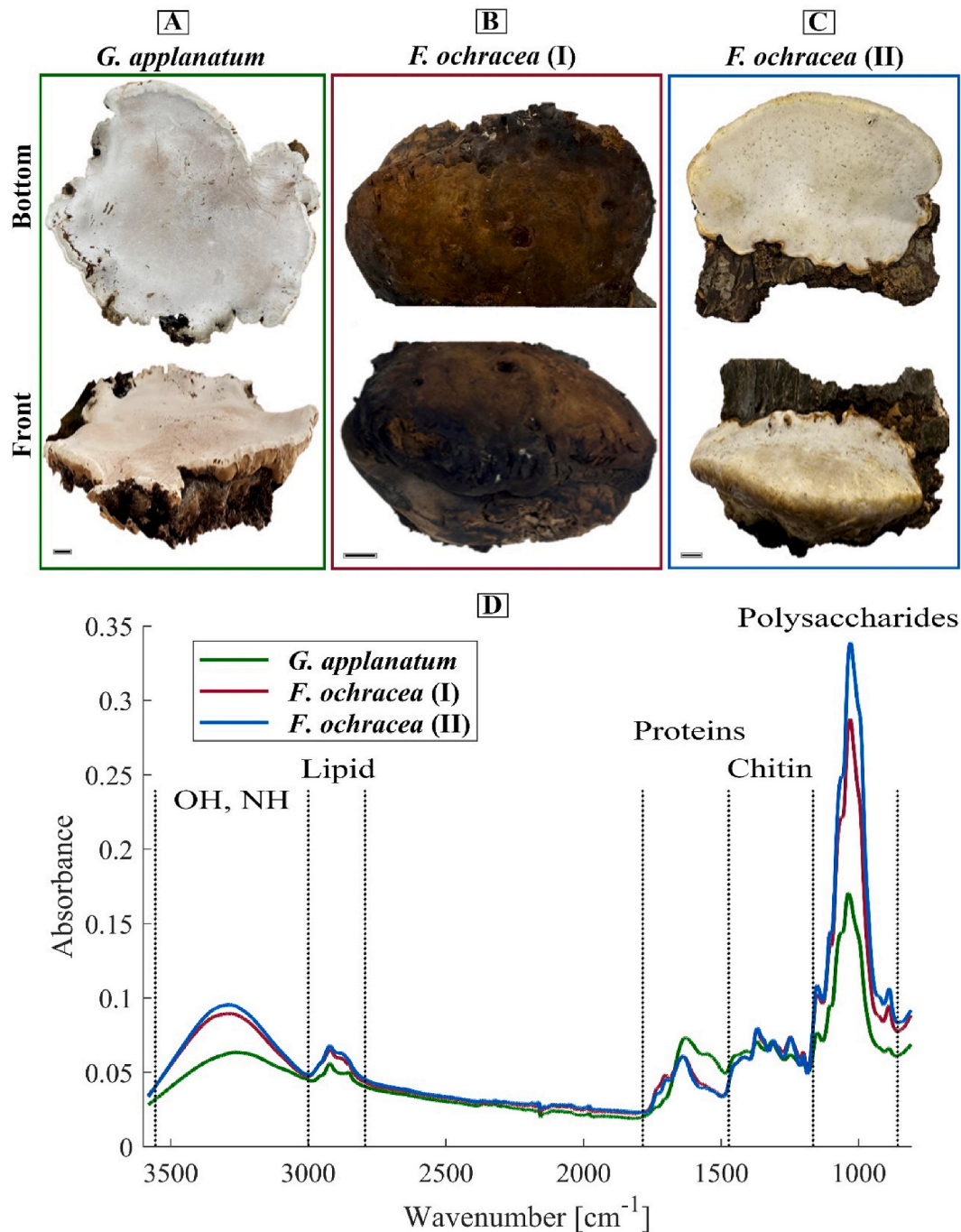
Fig. 2. Images of the three sporocarps of bracket fungi used in the study and their chemical composition, using Fourier-transform infrared spectroscopy (FTIR). **(A)–(C)** show images of the bottom and front views of *G. applanatum*, *F. ochracea* (I), and *F. ochracea* (II), respectively. All scale bars = 1 cm. **(D)** shows the chemical composition data ($n = 1$), where all chemical components in fungi are present in the three studied bracket fungi.

in two groups for each of the three bracket fungi sporocarps and the data is displayed in Fig. 3. The ultimate tensile strength, σ_{uts}, was statistically significantly higher ($p < 0.05$) in the radial direction than the transverse direction for all three sporocarps, as shown in Fig. 3 (A). The mean of σ_{uts} in the radial direction was 154%, 123%, and 174% higher than in the transverse direction for *G. applanatum*, *F. ochracea* (I), and *F. ochracea* (II), respectively. Similarly, the elastic modulus, E, was also statistically significantly higher ($p < 0.01$) in the radial direction than the transverse direction, as seen in Fig. 3 (B). The mean of E in the radial direction was 318%, 212%, and 755% higher in the radial direction than the transverse direction for *G. applanatum*, *F. ochracea* (I), and *F. ochracea* (II), respectively. The results in Fig. 3 (A and B) are further reinforced by the

stress-strain curves for all tensile tests, as presented in Fig. 3 (C). The stress-strain curves of one representative test per group for each sporocarp in Fig. 3 (C) show the anisotropic mechanical behavior of the context layer. The radial direction shows a higher slope of E and a higher σ_{uts} before failure compared to the transverse direction, aligning with the results in Fig. 3 (A and B). These trends are evident in other fungi when studying the effects of the directionality when subjected to compression and tensile tests, further establishing the anisotropic behavior of fungi (Porter and Naleway, 2022; Müller et al., 2021; Pylkkänen et al., 2023; Klemm et al., 2024). Klemm et al. performed a compression test and reported the tube layer's compressive strength as 448% higher in the radial direction than the transverse for the bracket
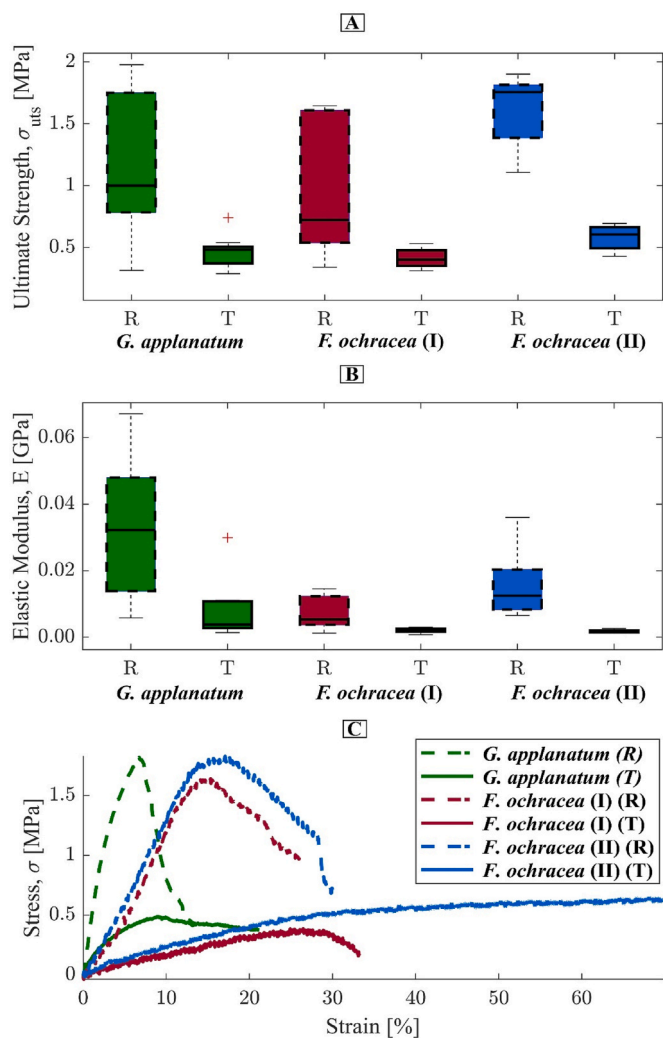
Fig. 3. Box and whisker plots (**A**–**B**) and stress-strain curves (**C**) for all tensile tests comparing the context layer's (**A**) ultimate tensile strength, σ_{uts}, and (**B**) elastic modulus, E, for each of the three bracket fungi sporocarps and testing orientations ($n = 9$): radial (R) and transverse (T). The R direction is statistically significantly higher ((**A**): $p < 0.05$ and (**B**): $p < 0.01$) than the T direction for all three sporocarps. (**C**) The stress-strain curves of one test per group for each sporocarp show the anisotropic, direction-dependent mechanical behavior leading to higher σ_{uts} and E in the R direction.

fungus, *Fomes fomentarius* (Klemm et al., 2024). Müller et al. also reported higher strength from a compression test for the tube layer in the radial direction for the hydrated *Fomes fomentarius*, where the average compressive strength was 550% more than the transverse direction (Müller et al., 2021). Pylkkänen et al. reported the compressive strength of the tube and the context layers, where they showed a 300% and 195% higher strength for the radial direction for the tube and context layers, respectively (Pylkkänen et al., 2023). Furthermore, Pylkkänen et al. (2023) also reported the mean ultimate tensile strength, σ_{uts}, and elastic modulus, E, for the context layer as 5.8 MPa and 0.3 GPa, respectively. When comparing these values to the current results for σ_{uts} (1.2, 0.93, and 1.60 MPa) and E (0.33, 0.0772, and 0.1548 GPa) for all three sporocarps tested, similar trends were observed despite the tests having been conducted on a wide variety of bracket fungus species. Other well-studied fungi species such as *Pleurotus eryngii*, *Agaricus bisporus*, *Pleurotus* spp., and *Lentinula edodes* also exhibit an anisotropic mechanical behavior and a change in the behavior of the stress-strain curve resulting in direction-dependent σ_{uts} and E (Porter and Naleway, 2022; Ogawa et al., 2012; McGarry and Burton, 1994). In *Pleurotus eryngii*, the

load-compression ratio curves for the stipe also showed a dependence on the growth direction for the mechanical behavior where the perpendicular (i.e., radial) direction for the upper part of the stipe and the lower part of the stipe exhibit a maximum force of 200% and 75% higher than the parallel (i.e., transverse) direction, respectively (Ogawa et al., 2012). *Agaricus bisporus* exhibits a 431% increased E in the stipe's longitudinal direction versus the transverse direction (McGarry and Burton, 1994).

3.3.2. Strain to failure

In contrast to σ_{uts} and E results, the strain to failure, ε_f, was statistically significantly lower ($p < 0.002$) in the radial direction than the transverse direction for all three sporocarps, as shown in Fig. 4. The ε_f in the transverse direction showed a mean percent increase as compared to the radial direction of 158%, 52%, and 168% for *G. applanatum*, *F. ochracea* (I), and *F. ochracea* (II), respectively. The stress-strain curves of all the tensile tests in Fig. 3 (C) show the statistically significant increase in strain in the transverse direction as compared to the radial direction. These results suggest the bracket fungi experience more strain while stretching in the transverse direction to absorb more energy. Pylkkänen et al. (2023) showed the mean strain to failure, ε_f, for the context layer from a tensile test as 4.3%, lower than the current results, ranging from 9.7% to 51%. However, they highlighted the complicated behavior they experienced during their tests, including an initial failure not experienced in the current tests.

3.3.3. Toughness

The absorbed energy during deformation, known as toughness, exhibits no statistically significant difference ($p > 0.25$) between the radial and transverse directions for all three bracket fungi sporocarps as seen in Fig. 5. The results in Fig. 5 suggest that although the bracket fungi demonstrate an anisotropic behavior for σ_{uts}, E, and ε_f, the energy required to deform the bracket fungi is the same regardless of the growth direction or loading alignment orientation. Because of the fungi's structure, the mechanical properties are complex, similar to other biological materials with complex structures, such as bone, skin, wood, and nacre (Naleway et al., 2015; Ha and Lu, 2020). The current toughness results from the three bracket fungi sporocarps average 0.34–0.880 MJ/m^3, which align with published toughness results on the context layer of another bracket fungus, *Fomes fomentarius*, averaging 0.2 MJ/m^3 (Pylkkänen et al., 2023). Critically, these toughness results demonstrate that, despite the anisotropy in the σ_{uts}, E, and ε_f data, these properties are able to balance in a way that provides directional isotropy in the energy necessary for failure in bracket fungi sporocarps.
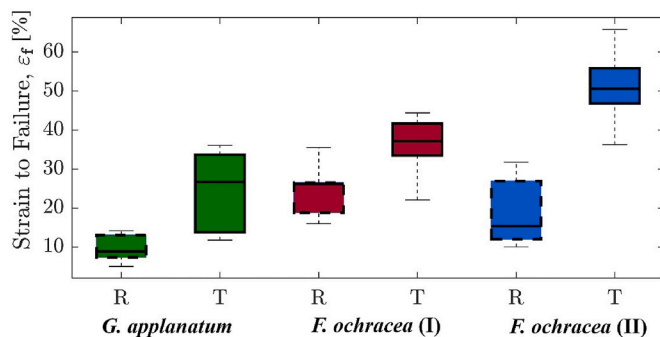
Fig. 4. Box and whisker plots comparing the context layer's strain to failure, ε_f, for each of the three bracket fungi sporocarps, and testing orientations ($n = 9$): radial (R) and transverse (T). The R direction is statistically significantly lower ($p < 0.002$) than the T direction for all three sporocarps.
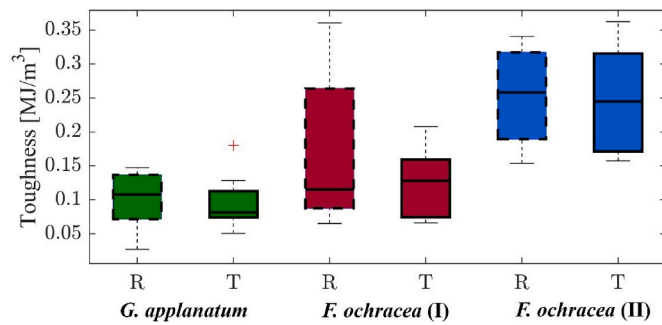
Fig. 5. Box and whisker plots comparing the context layer's toughness for each of the three bracket fungi sporocarps and testing orientations ($n = 9$): radial (R) and transverse (T). There is no statistically significant difference ($p < 0.05$) between the R and T orientations for all three sporocarps.

3.4. Microstructure imaging analysis

3.4.1. Pre-test characterization

The dense hyphae network in the context layer demonstrates a preferred orientation alignment for the three bracket fungi sporocarps, as shown by the SEM images and the histograms in Fig. 6. As visualized in Fig. 6 (A–C), Fig. 6 (D) shows approximately 60% of *G. applanatum*'s hyphae, 87% of *F. ochracea* (I)'s hyphae, and 66% of *F. ochracea* (II)'s hyphae are oriented within the $-15°$ to $15°$ range, with the majority of the hyphae aligning around $0°$, which corresponds to the radial direction. The clear alignment in the context layer elucidates the anisotropic mechanical behavior for σ_{uts}, E, and ε_f shown in Figs. 3 and 4. Of note, previous literature that studied the bracket fungi's context also indicated a preferential orientation alignment at the hyphae network scale, pointing to the radial direction (Porter and Naleway, 2022; Pylkkänen et al., 2023).

The context's hyphae diameter measurements shown in Fig. 7 (A) were statistically significantly different ($p < 0.02$) between all three bracket fungi sporocarps. Different fungi species have previously been shown to have different hyphae diameters (Pylkkänen et al., 2023; Bartnicki-Garcia et al., 2018), therefore these current results are not surprising. Although the diameters differ statistically significantly between bracket fungi sporocarps, the mechanical behavior trend is the same, as shown in Figs. 3 and 4. The context's hyphae density measurements shown in Fig. 7 (B) were only statistically significantly different between *G. applanatum* and *F. ochracea* (II) ($p < 0.01$). All three bracket fungi's hyphae networks were dense, with the median points of the % area the hyphae occupy being 77%, 92%, and 91% for *G. applanatum*, *F. ochracea* (I), and *F. ochracea* (II). Bracket fungi, which
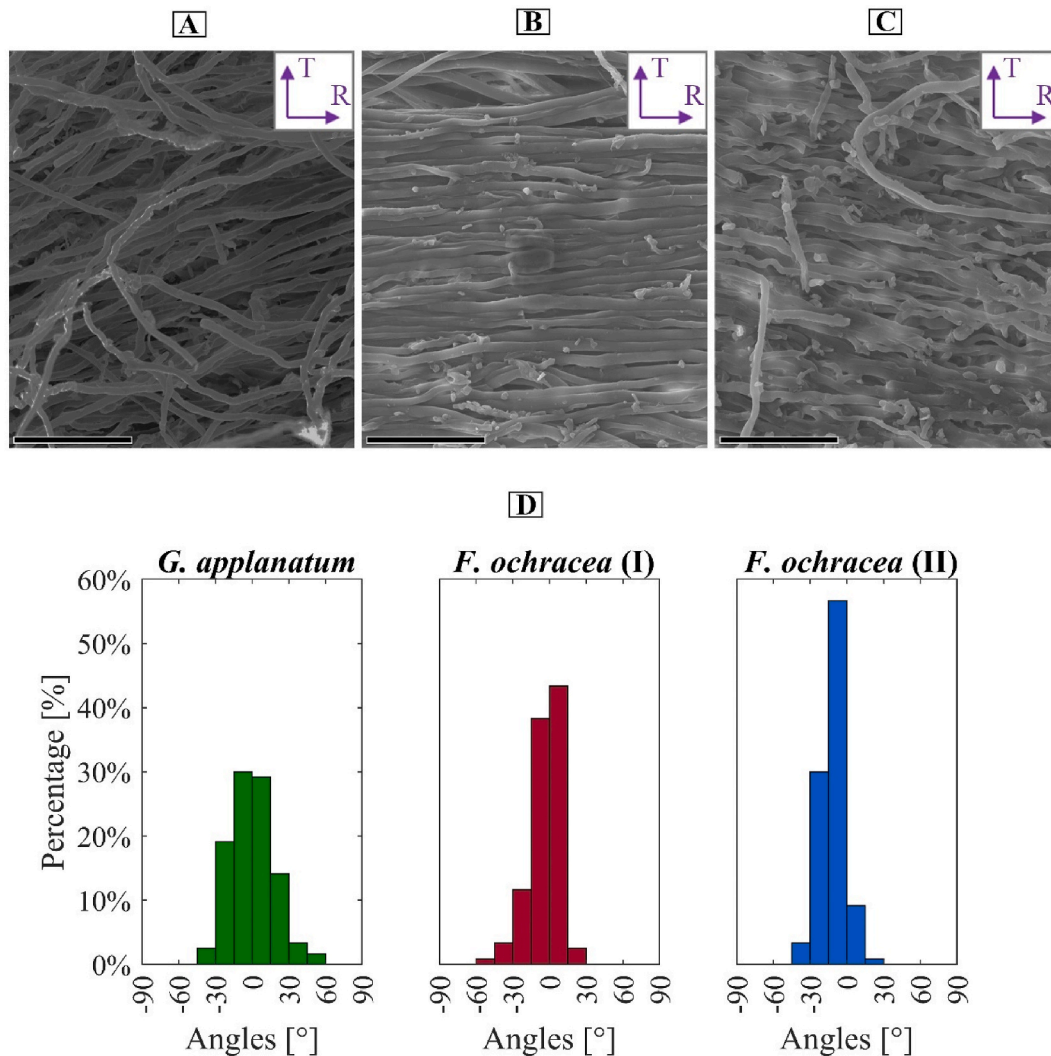
Fig. 6. Representative SEM images of the alignment orientation in the hyphal network in the context layer and their distribution before mechanical testing. **(A)**–**(C)** show representative SEM images of *G. applanatum*, *F. ochracea* (I), and *F. ochracea* (II), respectively. All scale bars = 50 μm. **(D)** shows histograms of the measured percent alignment orientation distribution for all three bracket sporocarps ($n = 120$), where $0°$ represents the radial direction.
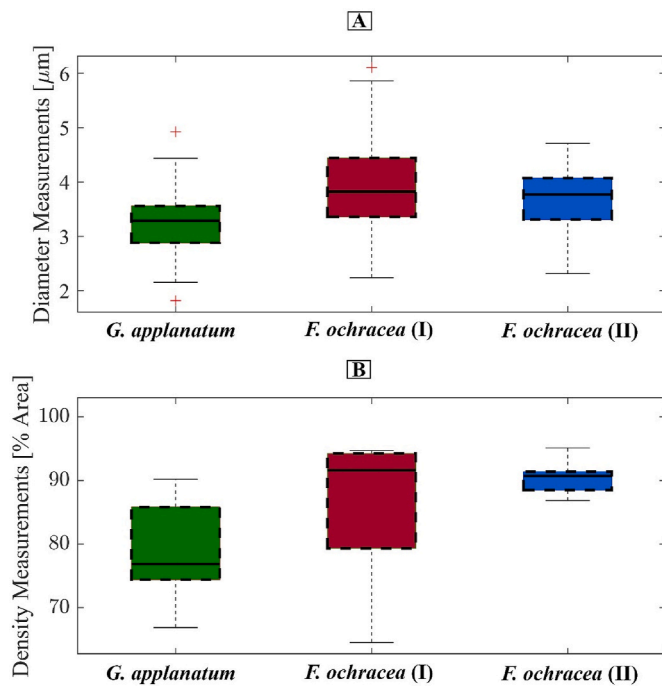
Fig. 7. Box and whisker plots comparing the context layer's **(A)** hyphae's diameter measurements ($n = 120$) and **(B)** hyphae's density measurements ($n = 6$) for each of the three bracket fungi sporocarps. **(A)** shows the hyphae's diameter measurements are statistically significantly different between the three sporocarps ($p < 0.02$). **(B)** shows the hyphae's density measurements are only statistically significantly different ($p < 0.01$) between *G. applanatum* and *F. ochracea* (II).

have a trimtic hyphal system, tend to be the densest of all fungi due to having all types of hyphae in their hyphal network (Porter and Naleway, 2022; Kirk et al., 2008), which aligns with these current results.

3.4.2. Post-test characterization

The anisotropic mechanical behavior for higher σ_{uts} and E is explained by the pre-test hyphal alignment in the radial direction; however, it does not explain the increase in deformation in the transverse direction, as shown by ε_f in Fig. 4. Examining the transverse direction samples after mechanical testing via SEM indicated that the hyphae network lost the preferential alignment shown in Fig. 6. The hyphae network, after testing, is exhibiting a chaotic distribution, without preference towards the 90° transverse direction as visualized in Fig. 8 (A–C) and demonstrated in the data in Fig. 8 (D). The chaotic distribution suggests the hyphae changed and sacrificed their alignment while deforming, which increased the energy absorption by deforming the samples statistically significantly more before failure, as shown in Fig. 4. This change in the network alignment to absorb more energy is seen in other biological materials, such as collagen fibrils and spider silk, where the fibers uncoil and slide during deformation under tension (Rosenberg et al., 2023; Elnunu et al., 2024; Piorkowski et al., 2020), suggesting a similar process here.

3.5. Bracket fungi biomechanical behavior

The three examined sporocarps of bracket fungi, *G. applanatum*, *F. ochracea* (I), and *F. ochracea* (II), showed consistent mechanical and microstructural behaviors, which aligned with previous reports thus suggesting that all bracket fungi have the same mechanical and microstructural trends and behaviors, which are governed by the alignment and directionality of their hyphae. This was further supported by the FTIR data, which demonstrated that there were no significant changes in the chemical composition of the three sporocarps, and the lack of

substantial variation in the hyphae diameter and density, both of which suggest that the observed results can be primarily attributed to the hyphae alignment. The mechanical data substantiated that bracket fungi are able to provide a balanced approach to their mechanical properties with varying anisotropic mechanical behavior in σ_{uts}, E, and ε_f, that results in isotropic toughness. This mechanical behavior can be attributed to a proposed model (diagrammed in Fig. 9) for the bracket's microstructural behavior when stressed. This model suggests that the hyphae's alignment within the context is related to the bracket's growth (with hyphae aligned in the growth direction, Fig. 9 (A–C)) and that, when strained in the transverse direction, these hyphae can reorient into a chaotic pattern, thus allowing for increased toughness and energy absorption before failure (Fig. 9 (D and E)). The energy absorption is evident in the fractured samples after the tensile test, where the samples exhibit signs of crack bridging and fiber pull-out, as shown in Fig. 8 (E). The bracket fungi growth behavior is unique and offers advantages to adapt and release spores efficiently. Bracket fungi's shelf-like structure growing outward from the tree trunk allows for maximizing the fungus' surface area to absorb nutrients from the tree trunk (Ginns, 2017). Some bracket fungi, such as *G. applanatum*, are perennial, which requires the fungi to grow and absorb more nutrients from the host efficiently (Mawar and Ram, 2020). The bracket fungi's anisotropic mechanical behavior allows for growing outward from the tree trunk. The hyphae's preferred radial alignment allows for the necessary mechanical advantage for the bracket fungi to grow radially to form a large shelf-like structure. The isotropic mechanical behavior protects the bracket fungi from deformation, i.e., damage. Because the bracket fungi grow outward from the tree, various weather conditions and predators may cause damage to the fungus with varying forces from different directions (Watkinson et al., 2015). Therefore, the deformation absorption in an isotropic manner allows for better damage-resistant properties. Despite the low E and σ_{uts}, the bracket fungi's lightweight, porous, and damage-resistant properties make it a viable alternative to existing fragile materials used in aerospace applications, such as aerogels (Porter et al., 2023).

4. Conclusions

This work utilized uniaxial tensile mechanical testing and microstructure imaging to study three sporocarps from two different species of bracket fungi and describe their context layer's material and mechanical behavior. This work allows an understanding of bracket's context layer in general rather than in specific species.

- The bracket sporocarps exhibit anisotropic mechanical behavior in their strength, elastic modulus, and strain to failure. The bracket fungi's ultimate strength and elastic modulus increased statistically significantly ($p < 0.05$ and $p < 0.01$) along the radial direction versus the transverse direction in all three tested sporocarps. In contrast, the strain to failure was significantly lower ($p < 0.002$) in the radial direction than the transverse direction.
- Energy is absorbed in an isotropic manner, as shown by the toughness, revealing no statistically significant difference between the tested samples in bracket's radial and transverse directions.
- The hyphae's dense network, which makes up the body of filamentous fungi and, in this case, bracket sporocarps, shows a clear alignment of the hyphae. The hyphae's alignment is primarily responsible for the anisotropic, direction-dependent mechanical properties.
- When strained, the hyphae's network realigns to form a more chaotic, less aligned distribution during uniaxial tensile testing against the alignment direction, providing more strain and energy absorption before failure.
- Bracket context mechanical properties and microstructural measurements are related to the alignment of hyphae. The bracket fungi utilize this alignment in growing large shelf-like structures radially
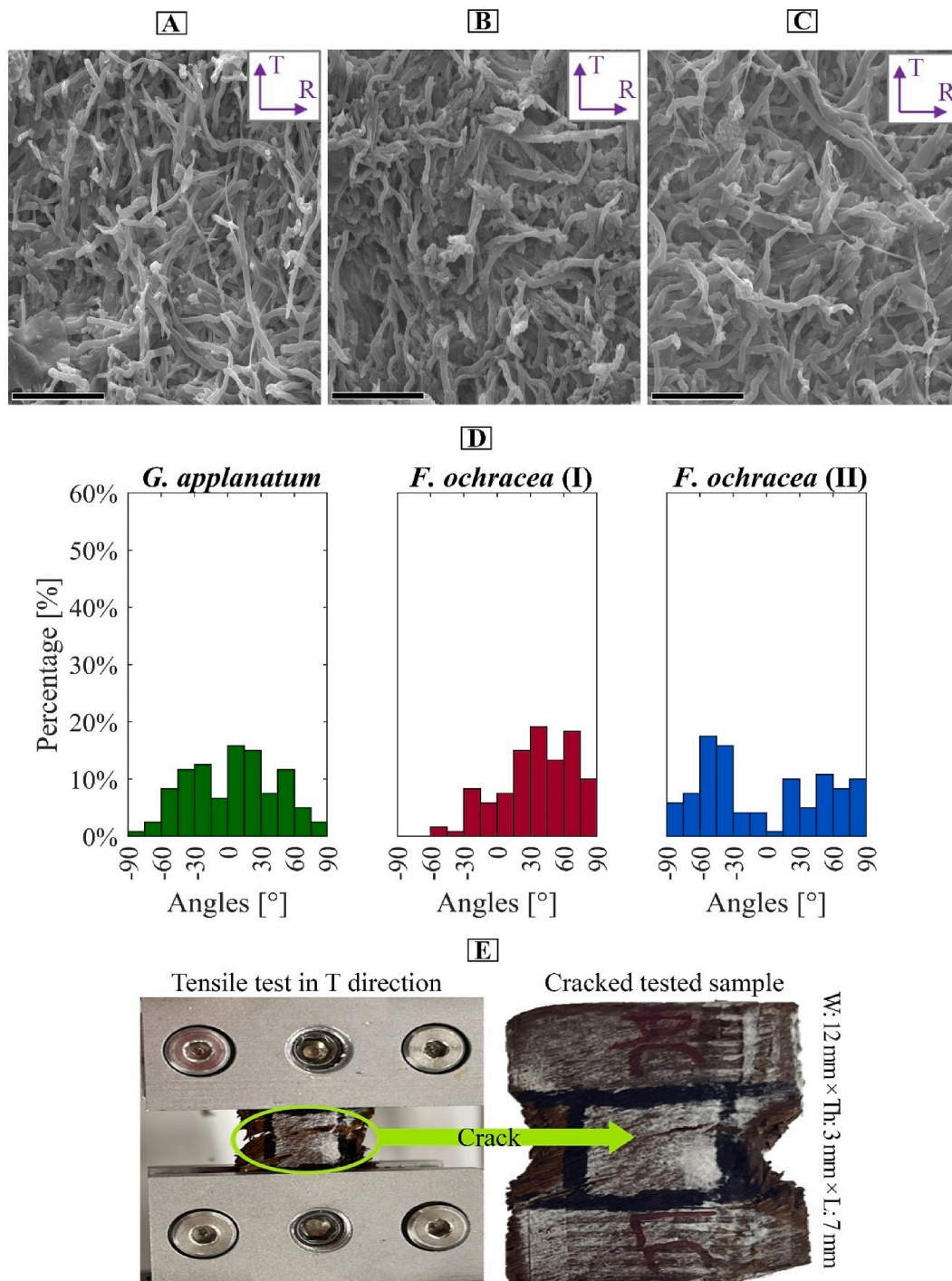
Fig. 8. Representative SEM images of the alignment orientation in the hyphal network in the context layer, their distribution after mechanical testing for the transversely mechanically tested samples, and the fracture behavior after testing. The SEM images and data are from the region between the clamp and the fracture point for the transverse orientation samples. **(A)–(C)** show representative SEM images of *G. applanatum*, *F. ochracea* (I), and *F. ochracea* (II), respectively after mechanical testing. All scale bars = 50 μm. **(D)** shows histograms of the measured percent alignment orientation distribution for all three bracket fungi sporocarps (n = 120), where 0° represents the radial direction. **(E)** shows the fracture behavior of the transversely tested samples after the tensile test.

from a tree. The context also offers a necessary mechanical advantage of damage resistance by absorbing the deformation from various weather and predator forces from all directions in an isotropic manner.

CRediT authorship contribution statement

Ihsan.S. Elnunu: Writing – review & editing, Writing – original draft, Methodology, Investigation, Formal analysis, Data curation, Conceptualization. **Jessica.N. Redmond:** Writing – review & editing, Data curation. **Bryn.T.M. Dentinger:** Writing – review & editing, Supervision, Funding acquisition. **Steven.E. Naleway:** Writing – review & editing, Supervision, Funding acquisition, Conceptualization.
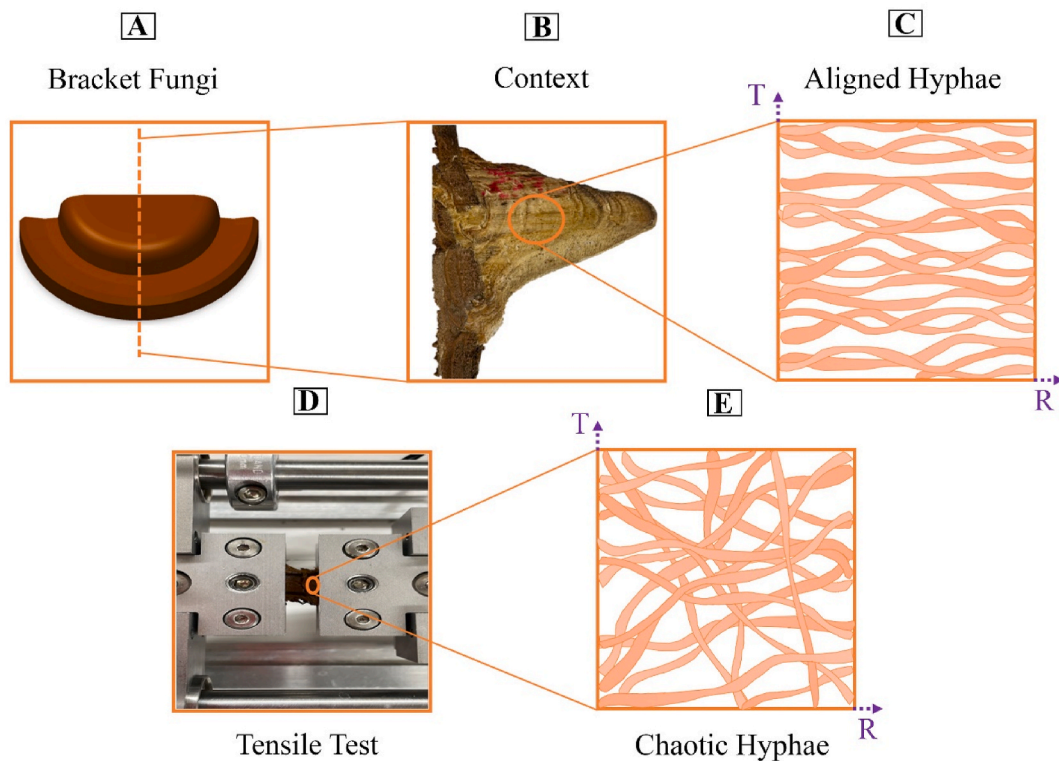
Fig. 9. Demonstration of the effect of uniaxial tensile mechanical testing on the bracket fungi's context layer's microstructural hyphal alignment. The bracket fungi's context layer loses the preferential radial alignment after undergoing a tensile test in the transverse direction. **(A)** Bracket fungi representative model. **(B)** cross-section of the bracket fungus' context. **(C)** representation of the hyphae's alignment in the context layer at the microstructure. **(D)** tensile test on transverse orientation sample. **(E)** representative of the hyphae's chaotic distribution after the tensile test for the transverse orientation group.

Disclaimer

Any opinions, findings, and conclusions or recommendations expressed in this material are those of the author(s) and do not necessarily reflect the views of the National Science Foundation.

Declaration of competing interest

The authors declare that they have no known competing financial interests or personal relationships that could have appeared to influence the work reported in this paper.

Acknowledgements

Appendix A. Supplementary data

Supplementary data to this article can be found online at https://doi.org/10.1016/j.jmbbm.2024.106841.

Data availability

Data will be made available on request.

References

Amobonye, A., Lalung, J., Awasthi, M.K., Pillai, S., 2023. Fungal mycelium as leather alternative: a sustainable biogenic material for the fashion industry. Sustain. Mater. Technol. 38, e00724. https://doi.org/10.1016/j.susmat.2023.e00724.

Bartnicki-Garcia, S., Garduño-Rosales, M., Delgado-Alvarez, D.L., Mouriño-Pérez, R.R., 2018. Experimental measurement of endocytosis in fungal hyphae. Fungal Genet. Biol. 118, 32–36. https://doi.org/10.1016/j.fgb.2018.07.001.

Bishop, K.S., 2020. Characterisation of extracts and anti-cancer activities of Fomitopsis pinicola. Nutrients 12, 609. https://doi.org/10.3390/nu12030609.

Bradshaw, A.J., Backman, T.A., Ramírez-Cruz, V., Forrister, D.L., Winter, J.M., Guzmán-Dávalos, L., Furci, G., Stamets, P., Dentinger, B.T.M., 2022. DNA authentication and chemical analysis of psilocybe mushrooms reveal widespread misdeterminations in fungaria and inconsistencies in metabolites. Appl. Environ. Microbiol. 88. https://doi.org/10.1128/aem.01498-22.

Bueno, D.J., Silva, J.O., 2014. FUNGI | the fungal hypha. In: Encyclopedia of Food Microbiology, second ed. Elsevier, pp. 11–19. https://doi.org/10.1016/B978-0-12-384730-0.00132-4.

Cheng, M., Zhang, L., Wang, J., Sun, X., Qi, Y., Chen, L., Han, C., 2024. The artist's conk medicinal mushroom Ganoderma applanatum (Agaricomycetes): mycological, mycochemical, and pharmacological properties: a review. Int. J. Med. Mushrooms 26, 13–66. https://doi.org/10.1615/IntJMedMushrooms.2024053900.

Cristini, V., Nop, P., Zlámal, J., Vand, M.H., Šeda, V., Tippner, J., 2023. Fomes fomentarius and F. Inzengae—a comparison of their decay patterns on beech wood. Microorganisms 11. https://doi.org/10.3390/microorganisms11030679.

Dentinger, B.T.M., Margaritescu, S., Moncalvo, J.M., 2010. Rapid and reliable high-throughput methods of DNA extraction for use in barcoding and molecular systematics of mushrooms. Mol. Ecol. Resour. 10, 628–633. https://doi.org/10.1111/j.1755-0998.2009.02825.x.

El-Enshasy, H.A., 2007. Filamentous fungal cultures – process characteristics, products, and applications. In: Bioprocessing for Value-Added Products from Renewable Resources. Elsevier, pp. 225–261. https://doi.org/10.1016/B978-044452114-9/50010-4.

Elnunu, I.S., Redmond, J.N., Obata, Y., Woolley, W., Kammer, D.S., Acevedo, C., 2024. Increased AGE cross-linking reduces the mechanical properties of osteons. JOM 76, 5692–5702. https://doi.org/10.1007/s11837-024-06716-x.

Elsacker, E., Vandelook, S., Brancart, J., Peeters, E., De Laet, L., 2019. Mechanical, physical and chemical characterisation of mycelium-based composites with different types of lignocellulosic substrates. PLoS One 14, 1–20. https://doi.org/10.1371/journal.pone.0213954.

Ghazvinian, A., Gürsoy, B., 2022. Mycelium-based composite graded materials: assessing the effects of time and substrate mixture on mechanical properties. Biomimetics 7, 48. https://doi.org/10.3390/biomimetics7020048.

Ginns, J., 2017. Polypores of British Columbia (Fungi: Basidiomycota).

Glen, M., Bougher, N.L., Francis, A.A., Nigg, S.Q., Lee, S.S., Irianto, R., Barry, K.M., Beadle, C.L., Mohammed, C.L., 2009. Ganoderma and Amauroderma species associated with root-rot disease of Acacia mangium plantation trees in Indonesia and Malaysia. Australas. Plant Pathol. 38, 345. https://doi.org/10.1071/AP09008.

Ha, N.S., Lu, G., 2020. A review of recent research on bio-inspired structures and materials for energy absorption applications. Compos. B Eng. 181, 107496. https://doi.org/10.1016/j.compositesb.2019.107496.

Haight, J.-E., Laursen, G.A., Glaeser, J.A., Taylor, D.L., 2016. Phylogeny of Fomitopsis pinicola: a species complex. Mycologia 108, 925–938. https://doi.org/10.3852/14-225R1.

Haight, J.-E., Nakasone, K.K., Laursen, G.A., Redhead, S.A., Taylor, D.L., Glaeser, J.A., 2019. Fomitopsis mounceae and F. schrenkii —two new species from North America in the F. pinicola complex. Mycologia 111, 339–357. https://doi.org/10.1080/00275514.2018.1564449.

Hattori, T., Sakayaroj, J., Jones, E.B.G., Suetrong, S., Preedanon, S., Klaysuban, A., 2014. Three species of Fulvifomes (Basidiomycota, Hymenochaetales) associated with rots on mangrove tree Xylocarpus granatum in Thailand. Mycoscience 55, 344–354. https://doi.org/10.1016/j.myc.2014.01.001.

Hawksworth, D.L., Lücking, R., 2017. Fungal diversity revisited: 2.2 to 3.8 million species. Microbiol. Spectr. 5, 79–95. https://doi.org/10.1128/microbiolspec.funk-0052-2016.

Islam, M.R., Tudryn, G., Bucinell, R., Schadler, L., Picu, R.C., 2017. Morphology and mechanics of fungal mycelium. Sci. Rep. 7, 1–12. https://doi.org/10.1038/s41598-017-13295-2.

Jeong, Y., Yang, B., Jeong, S., Kim, S., Song, C., 2008. Ganoderma applanatum : a promising mushroom for antitumor and immunomodulating activity. Phytother Res. 22, 614–619. https://doi.org/10.1002/ptr.2294.

Jo, W.-S., Cho, Y.-J., Cho, D.-H., Park, S.-D., Yoo, Y.-B., Seok, S.-J., 2009. Culture conditions for the mycelial growth of Ganoderma applanatum. MYCOBIOLOGY 37, 94. https://doi.org/10.4489/MYCO.2009.37.2.094.

Kauserud, H., Colman, J.E., Ryvarden, L., 2008. Relationship between basidiospore size, shape and life history characteristics: a comparison of polypores. Fungal. Ecol. 1, 19–23. https://doi.org/10.1016/j.funeco.2007.12.001.

Kaya, M., Akata, I., Baran, T., Menteş, A., 2015. Physicochemical properties of chitin and chitosan produced from medicinal fungus (Fomitopsis pinicola). Food Biophys. 10, 162–168. https://doi.org/10.1007/s11483-014-9378-8.

Kirk, P., Cannon, P., Minter, D., Stalpers, J., 2008. Ainsworth & Bisby's Dictionary of the Fungi, No. Ed. CABI, UK. https://doi.org/10.1079/9780851998268.0000.

Klemm, S., Freidank-Pohl, C., Bauer, A., Mantouvalou, I., Simon, U., Fleck, C., 2024. Hierarchical structure and chemical composition of complementary segments of the fruiting bodies of Fomes fomentarius fungi fine-tune the compressive properties. PLoS One 19, e0304614. https://doi.org/10.1371/journal.pone.0304614.

Luangharn, T., Karunarathna, S.C., Mortimer, P.E., Hyde, K.D., Xu, J., 2020. Morphology, phylogeny and culture characteristics of Ganoderma gibbosum collected from kunming. Yunnan Province, China, Phyton (B Aires) 89, 743–764. https://doi.org/10.32604/phyton.2020.09690.

Lücking, R., Aime, M.C., Robbertse, B., Miller, A.N., Aoki, T., Ariyawansa, H.A., Cardinali, G., Crous, P.W., Druzhinina, I.S., Geiser, D.M., Hawksworth, D.L., Hyde, K.D., Irinyi, L., Jeewon, R., Johnston, P.R., Kirk, P.M., Malosso, E., May, T.W., Meyer, W., Nilsson, H.R., Öpik, M., Robert, V., Stadler, M., Thines, M., Vu, D., Yurkov, A.M., Zhang, N., Schoch, C.L., 2021. Fungal taxonomy and sequence-based nomenclature. Nat. Microbiol. 6, 540–548. https://doi.org/10.1038/s41564-021-00888-x.

Luo, Q., Yang, X.-H., Yang, Z.-L., Tu, Z.-C., Cheng, Y.-X., 2016. Miscellaneous meroterpenoids from Ganoderma applanatum. Tetrahedron 72, 4564–4574. https://doi.org/10.1016/j.tet.2016.06.019.

Mawar, R., Ram, L., 2020. Deepesh, T. Mathur, Ganoderma. In: Beneficial Microbes in Agro-Ecology. Elsevier, pp. 625–649. https://doi.org/10.1016/B978-0-12-823414-3.00031-9.

McGarry, A., Burton, K.S., 1994. Mechanical properties of the mushroom, Agaricus bisporus. Mycol. Res. 98, 241–245. https://doi.org/10.1016/S0953-7562(09)80192-5.

Meyer, V., Basenko, E.Y., Benz, J.P., Braus, G.H., Caddick, M.X., Csukai, M., de Vries, R.P., Endy, D., Frisvad, J.C., Gunde-Cimerman, N., Haarmann, T., Hadar, Y., Hansen, K., Johnson, R.I., Keller, N.P., Kraševec, N., Mortensen, U.H., Perez, R., Ram, A.F.J., Record, E., Ross, P., Shapaval, V., Steiniger, C., van den Brink, H., van Munster, J., Yarden, O., Wösten, H.A.B., 2020. Growing a circular economy with fungal biotechnology: a white paper. Fungal. Biol. Biotechnol. 7, 5. https://doi.org/10.1186/s40694-020-00095-z.

Miettinen, O., Larsson, E., Sjökvist, E., Larsson, K.H., 2012. Comprehensive taxon sampling reveals unaccounted diversity and morphological plasticity in a group of dimitic polypores (Polyporales, Basidiomycota). Cladistics 28, 251–270. https://doi.org/10.1111/j.1096-0031.2011.00380.x.

Mohaček-Grošev, V., Božac, R., Puppels, G.J., 2001. Vibrational spectroscopic characterization of wild growing mushrooms and toadstools. Spectrochim. Acta Mol. Biomol. Spectrosc. 57, 2815–2829. https://doi.org/10.1016/S1386-1425(01)00584-4.

Money, N.P., Fischer, M.W.F., 2009. Biomechanics of spore release in phytopathogens. In: The Mycota. Springer Berlin Heidelberg, Berlin, Heidelberg, pp. 115–133. https://doi.org/10.1007/978-3-540-87407-2_6.

Müller, C., Klemm, S., Fleck, C., 2021. Bracket fungi, natural lightweight construction materials: hierarchical microstructure and compressive behavior of Fomes fomentarius fruit bodies. Appl. Phys. Mater. Sci. Process 127, 1–11. https://doi.org/10.1007/s00339-020-04270-2.

Naleway, S.E., Porter, M.M., McKittrick, J., Meyers, M.A., 2015. Structural design elements in biological materials: application to bioinspiration. Adv. Mater. 27, 5455–5476. https://doi.org/10.1002/adma.201502403.

Naranjo-Ortiz, M.A., Gabaldón, T., 2019. Fungal evolution: major ecological adaptations and evolutionary transitions. Biol. Rev. 94, 1443–1476. https://doi.org/10.1111/brv.12510.

Naumann, A., 2015. Fourier transform infrared (FTIR) microscopy and imaging of fungi. In: Dahms, T.E.S., Czymmek, K.J. (Eds.), J Chem Inf Model. Springer International Publishing, Cham, pp. 61–88. https://doi.org/10.1007/978-3-319-22437-4_4.

Ogawa, Y., Miyazawa, A., Yamamoto, N., Suzuki, A., 2012. Compression properties of the fruit body of king oyster mushroom Pleurotus eryngii. Int. J. Food Sci. Technol. 47, 2487–2492. https://doi.org/10.1111/j.1365-2621.2012.3126.x.

Ongpeng, J. Maximino C., Inciong, E., Sendo, V., Soliman, C., Siggaoat, A., 2020. Using waste in producing bio-composite mycelium bricks. Appl. Sci. 10, 5303. https://doi.org/10.3390/app10155303.

Petersen, J., 1987. Ganoderma in northern europe. Mycologist 1, 62–67. https://doi.org/10.1016/S0269-915X(87)80041-1.

Piorkowski, D., Blackledge, T.A., Liao, C.P., Joel, A.C., Weissbach, M., Wu, C.L., Tso, I.M., 2020. Uncoiling springs promote mechanical functionality of spider cribellate silk. J. Exp. Biol. 223. https://doi.org/10.1242/jeb.215269.

Porter, D.L., Naleway, S.E., 2022. Hyphal systems and their effect on the mechanical properties of fungal sporocarps. Acta Biomater. 145, 272–282. https://doi.org/10.1016/j.actbio.2022.04.011.

Porter, D.L., Hotz, E.C., Uehling, J.K., Naleway, S.E., 2023. A review of the material and mechanical properties of select Ganoderma fungi structures as a source for bioinspiration. J. Mater. Sci. 58, 3401–3420. https://doi.org/10.1007/s10853-023-08214-y.

Pylkkänen, R., Werner, D., Bishoyi, A., Weil, D., Scoppola, E., Wagermaier, W., Safeer, A., Bahri, S., Baldus, M., Paananen, A., Penttilä, M., Szilvay, G.R., Mohammadi, P., 2023. The complex structure of Fomes fomentarius represents an architectural design for high-performance ultralightweight materials. Sci. Adv. 9. https://doi.org/10.1126/sciadv.ade5417 eade5417.

Richter, C., Wittstein, K., Kirk, P.M., Stadler, M., 2015. An assessment of the taxonomy and chemotaxonomy of Ganoderma. Fungal Divers. 71, 1–15. https://doi.org/10.1007/s13225-014-0313-6.

Rosenberg, J.L., Woolley, W., Elnunu, I., Kamml, J., Kammer, D.S., Acevedo, C., 2023. Effect of non-enzymatic glycation on collagen nanoscale mechanisms in diabetic and age-related bone fragility. Biocell 47, 1651–1659. https://doi.org/10.32604/biocell.2023.028014.

Ryvarden, L., 2000. Studies in neotropical polypores 2: a preliminary key to neotropical species of Ganoderma with a laccate pileus. Mycologia 92, 180–191. https://doi.org/10.1080/00275514.2000.12061142.

Schmidt, B., Freidank-Pohl, C., Zillessen, J., Stelzer, L., Guitar, T.N., Lühr, C., Müller, H., Zhang, F., Hammel, J.U., Briesen, H., Jung, S., Gusovius, H.J., Meyer, V., 2023. Mechanical, physical and thermal properties of composite materials produced with the basidiomycete Fomes fomentarius. Fungal. Biol. Biotechnol. 10, 1–15. https://doi.org/10.1186/s40694-023-00169-8.

Schneider, C.A., Rasband, W.S., Eliceiri, K.W., 2012. NIH Image to ImageJ: 25 years of image analysis. Nat. Methods 9, 671–675. https://doi.org/10.1038/nmeth.2089.

Sterflinger, K., Tesei, D., Zakharova, K., 2012. Fungi in hot and cold deserts with particular reference to microcolonial fungi. Fungal. Ecol. 5, 453–462. https://doi.org/10.1016/j.funeco.2011.12.007.

ud-Din, F., Mukhtar, T., 2019. Morphological characterization of Ganoderma species from Murree hills of Pakistan. Plant Prot. 3, 73–84. https://doi.org/10.33804/pp.003.02.0128.

Valverde, M.E., Hernández-Pérez, T., Paredes-López, O., 2015. Edible mushrooms: improving human health and promoting quality life. Internet J. Microbiol. 2015, 1–14. https://doi.org/10.1155/2015/376387.

Vlasenko, V.A., 2013. Ecological characteristics of bracket fungi in the forest steppe of Western Siberia. Contemp Probl Ecol 6, 390–395. https://doi.org/10.1134/S1995425513040136.

Wang, X.-C., Xi, R.-J., Li, Y., Wang, D.-M., Yao, Y.-J., 2012a. The species identity of the widely cultivated Ganoderma, 'G. Lucidum' (Ling-zhi), in China. PLoS One 7, e40857. https://doi.org/10.1371/journal.pone.0040857.

Wang, X., Chen, X., Qi, Z., Liu, X., Li, W., Wang, S., 2012b. A study of Ganoderma lucidum spores by FTIR microspectroscopy. Spectrochim. Acta Mol. Biomol. Spectrosc. 91, 285–289. https://doi.org/10.1016/j.saa.2012.02.004.

Watkinson, S.C., Boddy, L., Money, N., 2015. The Fungi. Academic Press.

Wösten, H.A.B., 2019. Filamentous fungi for the production of enzymes, chemicals and materials. Curr. Opin. Biotechnol. 59, 65–70. https://doi.org/10.1016/j.copbio.2019.02.010.

Xing, J.-H., Sun, Y.-F., Han, Y.-L., Cui, B.-K., Dai, Y.-C., 2018. Morphological and molecular identification of two new Ganoderma species on Casuarina equisetifolia from China. MycoKeys 34, 93–108. https://doi.org/10.3897/mycokeys.34.22593.

Yoshimoto, C.M., 1970. A new species of astichus (hymenoptera: EULOPHIDAE) associated with the birch bracket fungus polyporus betulinus and woody fungus ganoderma applanatum in eastern Canada. Can. Entomol. 102, 656–659. https://doi.org/10.4039/Ent102656-6.

Zabel, R.A., Morrell, J.J., 2020. The characteristics and classification of fungi and bacteria. In: Wood Microbiology. Elsevier, pp. 55–98. https://doi.org/10.1016/B978-0-12-819465-2.00003-6.

Zhao, J., Lu, T., Pan, T., Li, X., Shi, M., 2022. Mushroom-shaped micropillar with a maximum pull-off force. J. Appl. Mech. 89, 1–9. https://doi.org/10.1115/1.4054628.

Zjawiony, J.K., 2004. Biologically active compounds from aphyllophorales (polypore) fungi. J. Nat. Prod. 67, 300–310. https://doi.org/10.1021/np030372w.